Chapter 6
Role of Thiolated layer
in Reduction of Energy Barrier

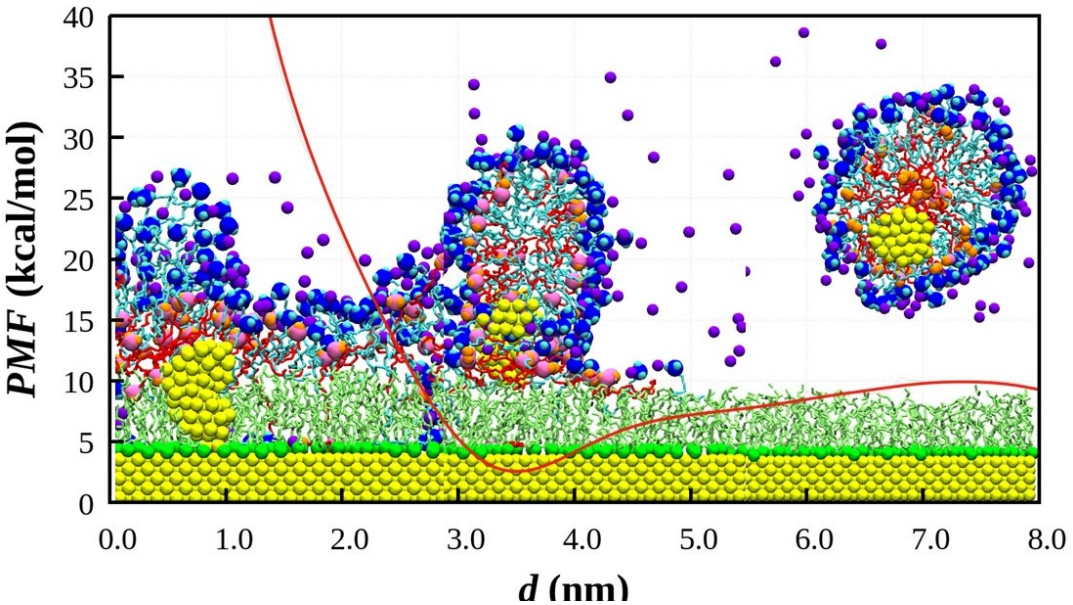

6.1 Introduction

Self-assembled monolayer (SAM) on solid substrates, formed by the adsorption of long-chain molecules through their head groups, represent a significant area of research due to their ability to create tunable surfaces with precisely defined size, shape, and composition. These molecular assemblies provide a versatile platform for fabricating functional surfaces with applications across various fields, including chemistry[215, 216], optics[217, 218], electronics[219], medicine[220], microfabrication[221, 222], and biology[223]. The properties of SAM, particularly those formed from alkanethiols, can be selectively modified by altering the functional groups at the head or tail while maintaining the overall chain conformation. This flexibility makes alkanethiol SAM highly adaptable for specific functional requirements. SAM can form on various solid substrates, such as

gold, silver, and silicon, through the spontaneous adsorption of molecules from a solution.[224] The exact arrangement and configuration of these molecules on the substrate surface have been debated for decades.

Self-assembly of surfactants depends strongly on the layering of water on a hydrophilic surface,[33, 225, 226] and they create aggregated structures. On the contrary, surfactants create a self-assembled monolayer under strong cohesive interactions between the hydrophobic tail group and the surface at lower coverage; whereas, at higher surface coverage, some of the surfactants leave the surface to create micelles at the bulk.[227] On a graphite surface, atomic force microscopy (AFM) image analysis indicates that sodium dodecyl sulfate (SDS) and cetyltrimethylammonium bromide (CTAB) tends to create a plane, hemispherical and hemicylindrical aggregates, parallel stripes based on the ionic strength and hemimicelles on a rough gold surface [228, 229]. The time required for equilibrium structure formation near the surface was also calculated [229].

Domínguez et al. studied self-aggregation of SDS on a graphite surface. At low surface coverage, SDS formed hemicylindrical aggregates, whereas, at high coverage, complete cylindrical structures emerged due to the formation of a water layer that created a hydrophilic environment. The SDS tails in cylinder-shaped structures were found to be straighter compared to those in hemicylinders.[34] Recently, Chowdhury et al.[156] have investigated the behaviour of sodium dodecyl sulfate (SDS) molecules at the mica/water interface and revealed the influence of temperature on the growth of self-assembled monolayers (SAM) of amphiphilic molecules, specifically n-octanol, and their impact on wetting behaviour and mass transfer dynamics on a mica surface.[230]

Recent studies have shed light on the structural arrangement of SAM, showing that sulfur atoms in alkanethiols bind to gold atoms on the substrate while the alkyl chains are closely packed and tilted at an angle of approximately 30° relative to the surface normal. Furthermore, exposing a gold surface to a solution containing a mixture of alkanethiols enables the formation of mixed SAM, where monolayers consist of a combination of gold-thiolate complexes.[59] This allows for the surface density of functional groups to be varied, offer-

ing additional opportunities for tailoring surface properties to specific applications. Ahn et al. demonstrated how SAM of alkyl thiols on gold surfaces evolves—from initial physisorption to densely packed layers.[37] Bhandary et al. have investigated the molecular dynamics of alkyl thiol adsorption on gold nanoparticles to form Janus nanoparticles with asymmetric surface coatings. The process involved a two-step mechanism, with thiol droplets initially binding to the gold surface ($\sim$ 1 ns) followed by diffusion-driven monolayer growth ($\sim$ 100 ns).[91]

In our previous study, the gold nucleates were stabilized within the micelle by favourable hydrophobic, electrostatic, and entropic interactions. However, the adsorption process faces resistance due to hydration layers and the need for micelle reorganization. The co-surfactant OLA was instrumental in reducing these challenges, enabling effective nucleate release and adsorption. Despite these improvements, a significant energy barrier persists, largely due to hydration layers and micelle reorganization requirements. Reducing this energy barrier is crucial for optimizing nucleation and growth processes. Therefore, we introduced sparingly dispersed thiol molecules on the gold surfaces and wanted to optimize the process via free energy estimation.

6.2 Models and Methodology

The simulation focused on modelling the formation of a sparingly dispersed thiol monolayer on a gold (111) surface using 1-hexadecane thiol (HT) molecules. Hexadecanethiol was modelled as a 16-carbon alkyl chain with a thiol headgroup, where CH_2 and CH_3

Table 6.1: Lennard-Jones (LJ) and Morse Potential Parameters of United Atoms

Nonbonded Interactions			
Atom	σ_{ij} **(Å)**	ϵ_{ij} **(kcal/mol)**	q **(e)**
CH_3	3.75	0.0914	0.0
CH_2	3.75	0.1947	0.0
CH_2(S)	3.75	0.1947	0.171
SH	3.62	0.461	-0.171
Morse	D_e **(kcal/mol)**	r_0 **(Å)**	α **(Å^{-1})**
Au-S	8.763	2.65	1.47

groups were treated as united atoms. The gold (111) surface consisted of three atomic layers in an FCC lattice and a lattice constant of 4.065 Å.

Initially, 108 HT molecules were randomly distributed on the gold surface. The simulations were conducted using a combination of force field parameters, including harmonic potentials for bond stretching and angle bending, and a triple cosine function to model torsion interactions, capturing the conformational flexibility of the alkyl chains. GROMOS96 53a6 forcefield[93] was used to model the bonded and non-bonded interactions for CTAB, OLA and HT molecules. An extended Simple Point Charge (SPC/E) water model was used to model the solvent. Non-bonded interactions were modelled using the Lennard-Jones (LJ) potential, while the sulfur-gold (S-Au) interaction was represented using a hybrid potential. This hybrid potential was employed by incorporating a Morse potential for distances below 4.4 Å, and an LJ potential for distances beyond 4.4 Å.[37] The LJ and Morse parameters for each atom are listed in Table 6.1. Lorentz-Berthelot (LB) combination rules were applied to calculate cross-interactions between heteroatomic pairs, ensuring consistent force field parameters.[214] The simulation used LJ parameters for gold atoms as reported by Heinz et al.[231] Periodic boundary conditions were employed in all three spatial directions to replicate an infinite system and minimize edge effects. Molecular dynamics simulations were carried out using LAMMPS[211], and VMD[150] was used to visualize the simulation trajectories.

To ensure system stability, the initial configuration underwent an energy minimization procedure using the steepest descent method for 5000 steps. This step reduced any unfavorable interactions and prepared the system for subsequent molecular dynamics simulations. After a 10 ns equilibration run, the HT molecules self-assembled into a monolayer on the gold surface, as shown in Figure 6.1(a). The sulfur atoms in the SH groups adsorbed strongly onto the gold surface, while the alkyl tails (CH_2 and CH_3 groups) oriented away from the surface, creating a hydrophobic layer on gold (111) surface.

The energy landscape for the fusion of nucleates with the gold surface was calculated using the umbrella sampling technique[155] followed by the Weighted Histogram Analysis

Method (WHAM) [154]. In the umbrella sampling, a series of 70 linearly spaced windows along the reaction coordinate, defined by the distance between the centre of mass of the nucleate and the apex of the gold surface, were subjected to an external biasing potential to facilitate comprehensive sampling within these windows. A harmonic potential, $u_i = \frac{1}{2}k(r - r_i)^2$ used as the external biasing potential at window i, where r_i represents the reference location and k denotes the harmonic force constant. We utilized the Weighted Histogram Analysis Method (WHAM) to remove the biasing potential and reconstruct the potential of mean force (PMF).[154] The reaction coordinate defined as the distance between the centre of mass of gold nucleate and the upper surface of the gold (111) surface was the reaction coordinate. A 1.0 ns production runs were conducted in an NVT ensemble for each window at 303.15 K, employing restraints with a harmonic force constant of 100 kcal/mol.Å^2. In WHAM, the calculation of PMF involved setting the number of bins to 100, accompanied by a tolerance for iterations of 10^{-5}. We monitored the size and shape of the micelle by calculating the components of the radius of gyration (R_g) tensor, $R_{g_{xx}}$, $R_{g_{yy}}$, $R_{g_{zz}}$, respectively. The radius of gyration R_g of the micelle was calculated using the equation: $R_g = \sqrt{(\sum_{i=1}^{N}(R_i - R_{COM})^2)/N}$ where, N is the total number of atoms in the micelle, R_{COM} is the center of mass (COM) of that micelle, and R_i is the position of the i^{th} atom in the micelle. We calculated the order parameter to understand the orientation of the molecules within the micelle on the gold surface. The order parameter of the micelle molecules is a measure of the degree of ordering and alignment of CTAB molecules within a micelle structure. The order parameter expressed as $S_{zz} = (3cos^2\theta_i - 1)/2$ where, θ_i is the angle between the end-to-end vector of the i^{th} molecule and the surface normal vector.

6.3 Result and Discussion

We have started our discussion with the density profile of water, micelle and thiol molecules along the z-dimension to understand the formation of the hydration layer by water molecules on the thiol layer, the distributions of thiol molecules on the surface.

Figure 6.1(a) depicts the functionalization of a gold (111) surface with hexadecanethiol

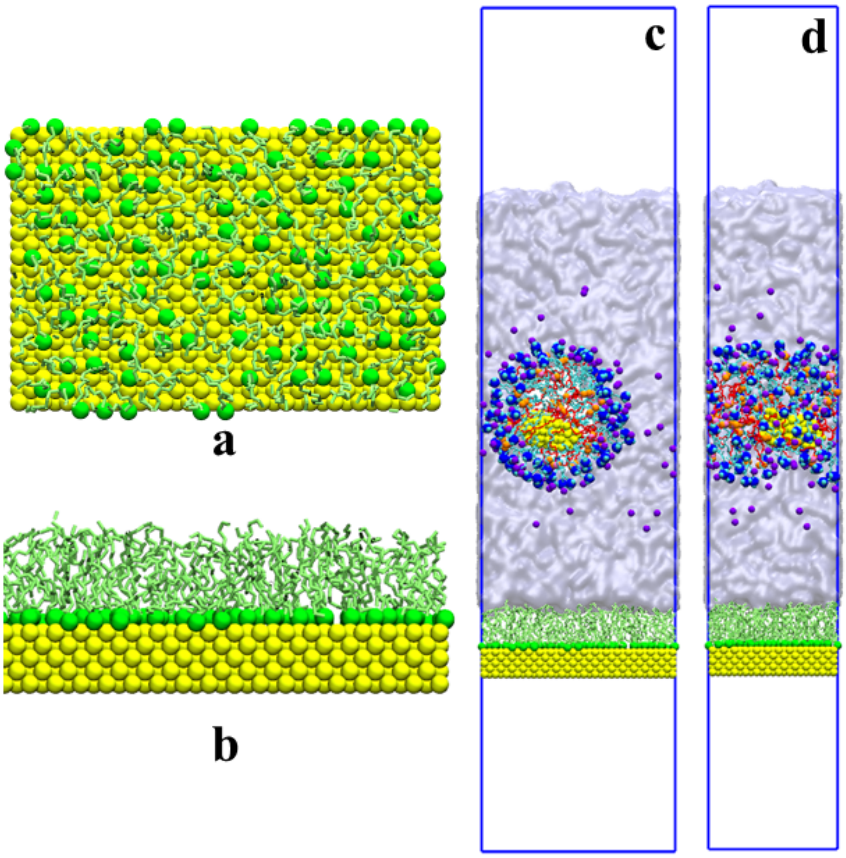

Figure 6.1: a, b – Dispersed hexadecane thiol monolayer on a gold (111) surface – top and side view, respectively. The thiol groups are represented as green spheres, respectively, and all the methyl groups are represented in green. c,d – Cross-sectional (xz-plane) and longitudinal (along y-axis) view, respectively, of the cylindrical micelle formed by CTAB and OLA. For CTAB molecules, the nitrogen atoms and bromide ions are represented as blue and purple spheres, respectively, and all the methyl groups are represented as cyan-colored bonds. For OLA molecules, the nitrogen atoms and hydrogen atoms are represented as pink and orange spheres, respectively, and all the methyl groups are represented as red-colored bonds. Water has shown an ice-blue colour in continuous media. The blue rectangle represents the periodic simulation box.

molecules. The thiol groups, responsible for bonding with the gold surface, are represented as green spheres, while the methyl groups of the alkyl chain are depicted in green, highlighting the formation of a hydrophobic monolayer on the surface. This functionalisation creates a structured interface that can influence the interactions with nearby molecules, such as surfactants and micelles. Figure 6.1(b) The front view of the hexadecane thiol monolayer shows the structural orientation of the thiol molecules on the gold (111) surface. The thiol molecules are aligned vertically, with their sulfur atoms bound to the gold surface and their methyl groups extending outward, creating a hydrophobic in-

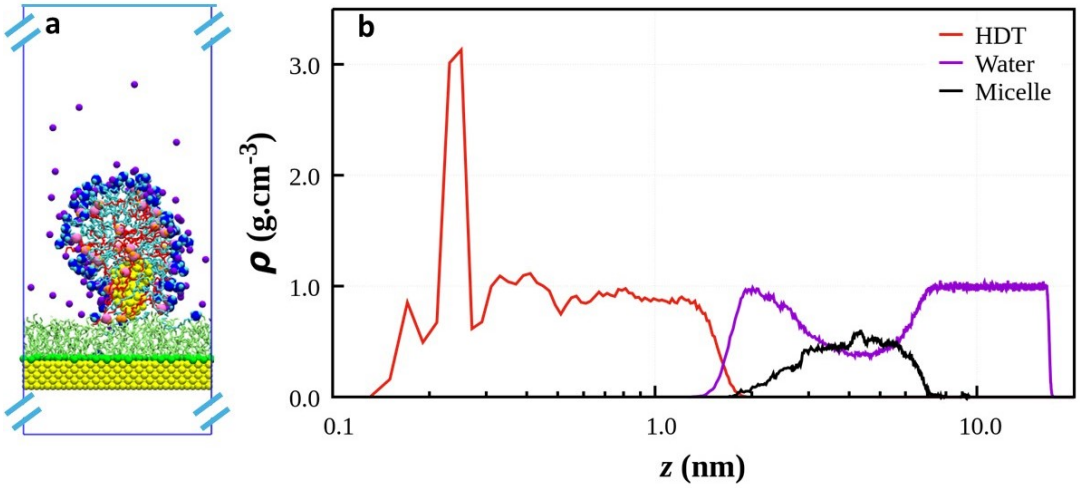

Figure 6.2: (a) Snapshot of the system containing a cylindrical micelle of co-surfactant OLA with CTAB molecules on the thiol-functionalized gold surface in an aqueous media. The Au(111) surface, at the bottom, is represented in yellow spheres. Water has shown an ice-blue color continuous media. The blue rectangle represents the periodic box (not to scale in the z-direction). (b) Density profile of water, micelle and thiol molecules along the z-axis

terface. This arrangement ensures the stability of the monolayer and provides a structured surface for interactions with the micelle. Figure 6.1(c) represents a cross-sectional view (xz-plane) of the cylindrical micelle formed by CTAB and OLA molecules after a production run. In this micelle, the nitrogen atoms of CTAB and bromide ions are shown as blue and purple spheres, respectively, while the methyl groups of CTAB are in cyan. Nitrogen and hydrogen atoms are depicted as pink and orange spheres for the OLA molecules, respectively, with the methyl groups in red. This visualisation revealed the spatial organisation of the micelle, where CTAB molecules form the outer shell, and OLA molecules occupy the core. Bromide ions stabilise the structure near the positively charged nitrogen headgroups of CTAB. Figure 6.1(d) shows the micelle system along the y-axis, providing a snapshot of the micelle interacting with the surrounding medium. The water molecules are depicted as a continuous ice-blue medium, showing how the micelle is suspended in an aqueous environment. The blue rectangle outlines the periodic simulation box used for molecular dynamics, replicating a bulk solution to ensure realistic modelling. This visualization highlights the micelle's structural stability and the dynamic interaction between its components and the surrounding solvent during the simulation.

Figure 6.2 (a) shows a snapshot of the system containing a cylindrical micelle of OLA co-surfactant with CTAB molecules on the thiol-functionalized gold surface in an aqueous medium. Figure 6.2 (b) depicts the density profiles of water, micelles, and thiol molecules along the z-axis, providing insight into their spatial distribution in the simulation system. The sharp peak represented by the red line near the surface (at ~ 0.2 nm) indicated that HDT molecules are strongly adsorbed onto the Au(111) gold surface. The water density profile represented by the blue line indicates that the density increases sharply near the thiol layer, indicating a hydration layer forming due to interactions with HDT molecules. The broadening of the water density near the micelle suggests the formation of a hydration layer. Beyond this region, the water density stabilises at a constant value, representing the bulk phase of water. The micelle density profile exhibits a distinct peak represented by the black line at ~ 4.25 nm, corresponding to the location of the micelle layer. The overlap between the red and blue curves suggested interactions between the micelle and surrounding water molecules. This interaction contributes to the hydration layer and micelle stability.

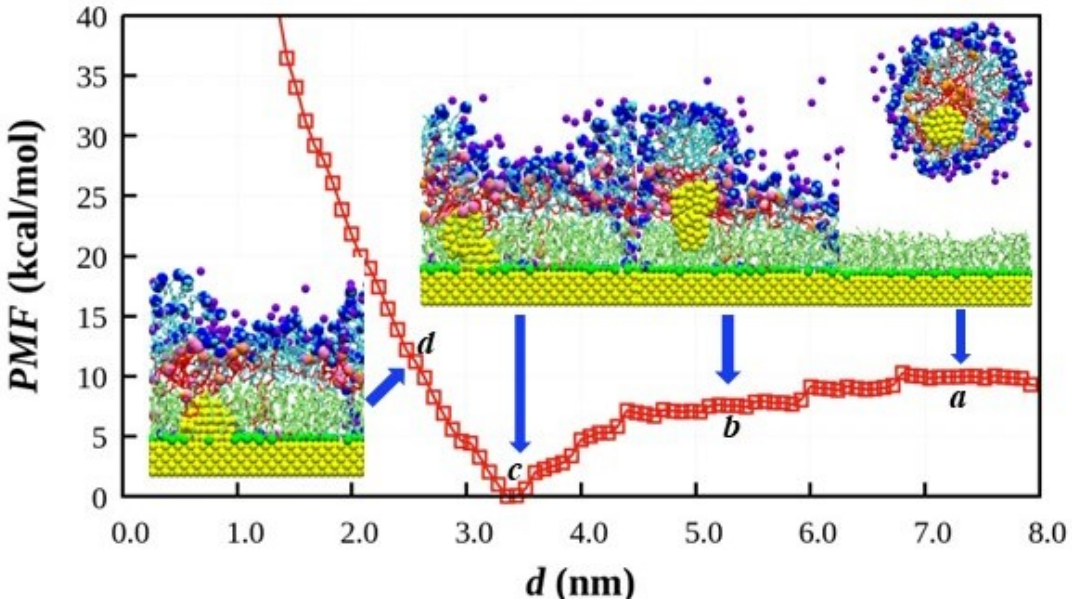

Figure 6.3: Potential of Mean Force (PMF) as a function of the distance (d) between the gold nucleate and the functionalized gold surface with hexadecane thiol molecules. Insets depict the structural configurations of the micelle containing gold nucleate at various stages along the reaction coordinate. The black arrows indicate the position of the nucleate from the apex of the thiolated layer on the gold surface. The color codes for molecular presentation are the same as in Figure 6.1, and water is omitted for visual clarity.

Figure 6.3 depicts the potential of mean force (PMF) profile for the interaction of a gold

nucleate encapsulated within a CTAB-OLA micelle with a hexadecanethiol-functionalised gold surface, providing critical insights into the energy landscape and structural evolution of the system during this process. At point "a" ($\sim$ 7.0 nm), the micelle resides in its most stable configuration in the bulk solvent. In this state, it retains its spherical integrity, and the encapsulated gold nucleate remains shielded by the surfactant molecules, with only weak long-range interactions (e.g., van der Waals forces) between the micelle and the surface. As the micelle moves closer to the thiolated layer on the gold surface, point "b" ($\sim$ 5.0–6.0 nm) marks the onset of steric and hydrophobic interactions imposed by the hexadecane thiol-functionalized surface. This leads to initial structural deformation of the micelle and an increase in PMF, reflecting the work required to overcome these interactions. At point "c" ($\sim$ 4.0 nm), the PMF reaches a local maximum, indicating the presence of a significant energy barrier. This energy barrier arises from the steric and hydrophobic effects of the dodecanethiol layer, which resist further approach of the micelle. Corresponding structural changes in the micelle include partial deformation, with the encapsulated gold nucleate remaining shielded but in closer proximity to the surface. Overcoming this energy barrier is a critical step that enables the micelle to transition to the near-surface interaction state. At point "d" ($\sim$ 2.5–3.0 nm), the PMF decreases sharply, signifying the formation of strong interactions between the micelle and the functionalized surface. At this stage, the micelle undergoes substantial deformation, flattening against the surface, and the surfactants rearrange to facilitate closer contact between the encapsulated gold nucleate and the gold surface. Strong van der Waals interactions dominate, stabilizing the system in a new energy minimum.

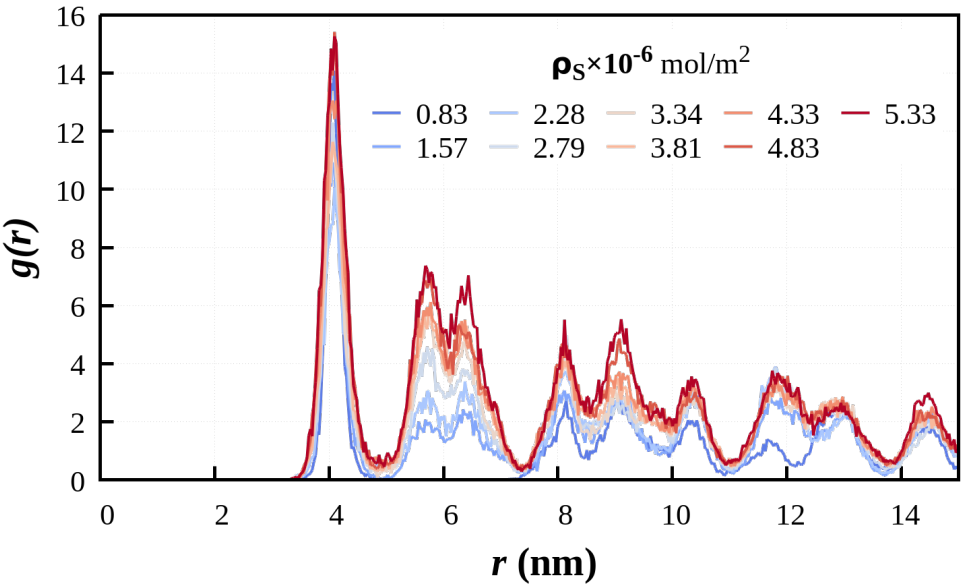

Figure 6.4: In-plane pair correlations (radial distribution function) between thiol molecules on Au(111) surface. Blue to red color gradient represents the RDF profiles at different surface densities of thiol molecules.

Figure 6.4 In-plane correlations (radial distribution functions) between thiol molecules adsorbed on an Au(111) surface. At low surface density of thiol molecules, the RDF shows fewer pronounced peaks, indicating a less ordered arrangement of molecules due to the larger spacing between them. As the surface density increases (blue to red), the peaks become more prominent and shift slightly, indicating tighter packing and enhanced ordering of the thiol molecules. At higher surface density of thiol molecules, the RDF shows sharper and more distinct peaks, suggesting increased molecular ordering as the molecules are packed more closely.

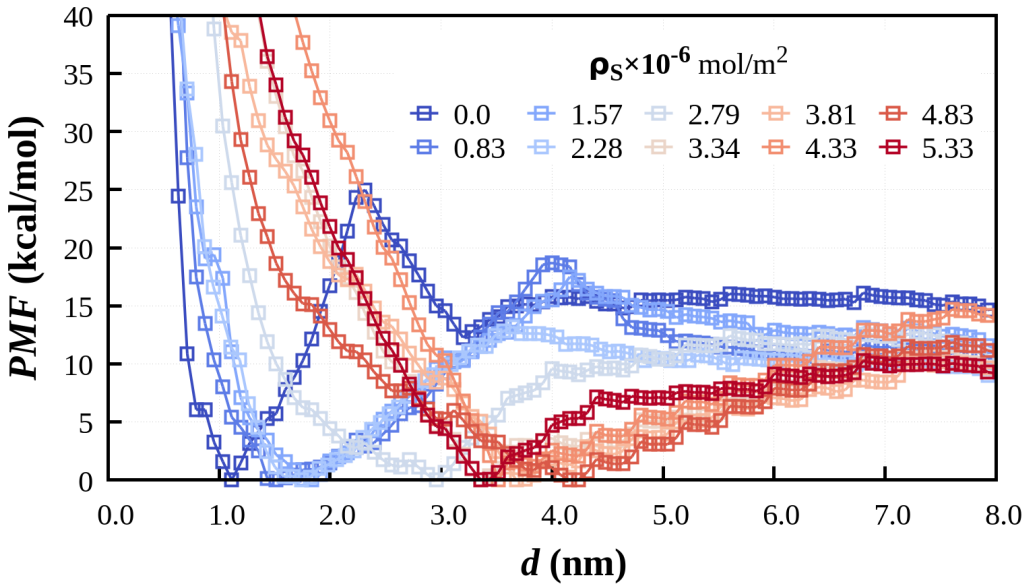

Figure 6.5: Potential of Mean Force (PMF) as a function of the distance (d) between the centre of mass of the gold nucleate and the thiol-functionalized gold surface for various surface densities of thiol molecules. Blue to red color gradient represents the PMF profiles at different surface densities of thiol molecules.

Figure 6.5 shows the effect of thiol surface density on the Potential of Mean Force (PMF) for the interaction between a gold nucleate encapsulated within a CTAB-OLA micelle and a thiol-functionalized gold surface. The PMF profiles, plotted as a function of the distance (d) between the centre of mass of the gold nucleate and the surface, show a clear trend: as the surface density of thiols (ρ_S) increases, the energy barrier decreases significantly. This reduction in the energy barrier is primarily attributed to the hydrophobic nature of the thiol layer, which facilitates stronger micelle-surface interactions and stabilizes the gold nucleates. At lower thiol densities, the PMF profiles exhibit steep energy barriers, indicating higher resistance to the micelle towards the thiolated layer. In contrast, higher thiol densities result in a downward shift of the PMF curves, reflecting reduced resistance and enhanced stabilization of the nucleate on the surface. The energy minimum observed at shorter distances ($\sim$ 2.0–3.0 nm) becomes more pronounced with increasing thiol density, representing the most stable configuration of the micelle and nucleate on the surface. This enhanced stabilization is due to stronger hydrophobic and steric interactions provided by the densely packed thiol layer.

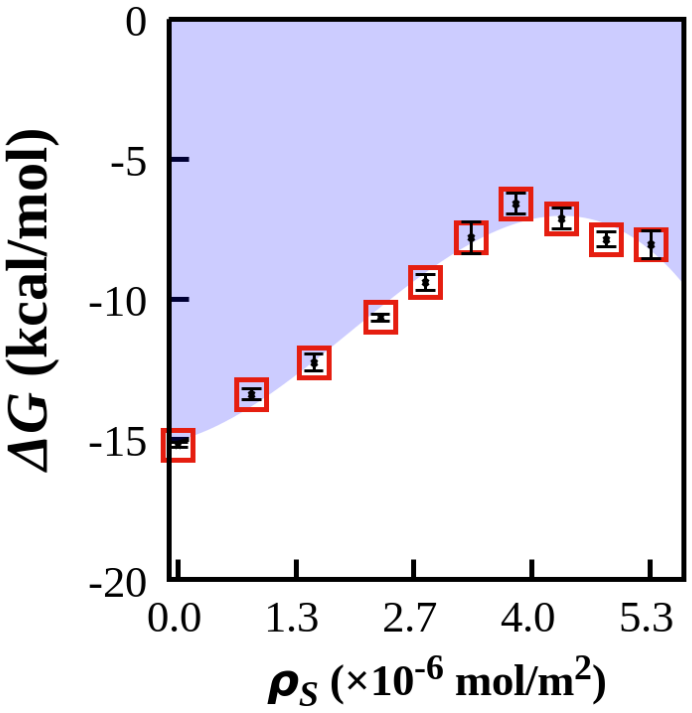

Figure 6.6: Change in free energy (ΔG) as a function of the surface density of thiol molecules (ρ_S)

Figure 6.6 illustrates the relationship between the change in free energy (ΔG) and the surface density of thiol molecules (ρ_S). The ΔG values remain negative throughout, indicating that the process is thermodynamically favorable at all thiol densities. However, as the surface density increases, there is a gradual decrease in the magnitude of ΔG, with the system reaching a plateau at higher thiol densities. The negative free energy values suggest that the introduction of a thiol layer significantly enhances the thermodynamic stability of thiol. This stabilization is primarily attributed to the hydrophobic interactions between the thiol molecules and the micelle, as well as the structural rearrangements within the micelle that optimize its interaction with the functionalized surface. As the thiol density increases, the more favorable interactions reduce the energy barrier for adsorption and nucleation, further facilitating the growth of gold nucleates on the surface. The plateau observed at higher thiol densities indicates a saturation effect, where further increases in thiol density provide diminishing returns in terms of free energy changes. The Optimum surface density is 3.34×10^{-6} mol/m^2.

6.4 Summary

This PMF profile highlights the critical role of surface functionalization in tuning the interaction dynamics between nanoparticles and surfaces. The introduction of the hexadecanethiol layer significantly increases the energy barrier compared to an unfunctionalized surface, demonstrating the importance of steric and hydrophobic effects in modulating interaction forces. These findings provide valuable insights into the molecular-level mechanisms governing nanoparticle-surface interactions and offer guidelines for designing functionalized surfaces to optimize nanomaterial synthesis and surface engineering. The thiol layer reduces the energy barrier; the Optimum surface density is 3.34×10^{-6} mol/m^2. This behavior highlights the importance of optimizing the thiol surface density to balance stability and efficiency during nanoparticle synthesis. Overall, the results underscore the critical role of surface functionalization in promoting thermodynamic favorability and facilitating micelle-mediated nucleation processes.